Turkish Journal of Electrical Engineering & Computer Sciences

http://journals.tubitak.gov.tr/elektrik/

Research Article

Turk J Elec Eng & Comp Sci
(2017) 25: 3645 – 3659

doi:10.3906/elk-1604-190

A reduced-order observer based on stator flux estimation with straightforward parameter identification for sensorless control of DFIGs

Rahim AJABI-FARSHBAF*, Mohammad Reza AZIZIAN, Vahid ESLAMPANAH
Department of Electrical Engineering, Sahand University of Technology, Tabriz, Iran

Received: 17.04.2016 • **Accepted/Published Online:** 17.02.2017 • **Final Version:** 05.10.2017

Abstract: This paper presents a new reducer-order observer for sensorless control of doubly fed induction generators (DFIGs), based on the Luenberger algorithm. Stable operation of the suggested observer is also considered in the design guidelines. Stator flux is selected as the state variable for the observer and its estimation error is used to correct the observer operation. The gain matrix of the proposed observer is calculated on the basis of flux error dynamics. The adaptation mechanism of the proposed observer is selected based on an estimation of rotor currents. A proportional integrator (PI) block is used in the structure of the adaptation mechanism for the transformation of its output signal. Furthermore, a fuzzy PI is designed to be applied to the observer structure, and a generalized study is carried out on the parameter estimation for the proposed observer. Simulation and practical results show the appropriate operation and speed tracking capability of the observer.

Key words: Doubly fed induction generator, parameter identification, reduced-order observer, speed sensorless control

1. Introduction

Generally, machine speed data are needed for implementing most control strategies, especially vector control [1–3]. Installation and maintenance of speed sensors in the wind turbines and generators are time-consuming and costly activities due to their large height. Therefore, sensor elimination leads to significant facilities. The main reasons for speed sensor elimination in most control methods are summarized as follows [1]:

1. The speed sensor renders the overall system complex and expensive.
2. In long-time operations, sensor failure is much more likely; therefore, sensorless control strategies are encouraged.
3. When a speed sensor fails, the controller receives incorrect feedback signals that disturb its operation. Therefore, a fault tolerance system must be designed. In fault diagnosis and tolerance (FDT) systems, in addition to sensor feedbacks, a speed estimation algorithm must be used for increasing system reliability.

Nowadays, speed estimation methods are extensively applied in the literature. Basic and fundamental algorithms are reviewed in ..[4] for induction machines (IMs). Several speed estimation algorithms for doubly fed induction machines (DFIMs) and doubly fed induction generators (DFIGs) are generally reviewed as follows. In [5], the basic structure of a model reference adaptive system (MRAS) algorithm was changed for application to

*Correspondence: r_ajabi@sut.ac.ir

sensorless control of DFIG. In [6], a senseless control strategy is developed on the basis of a phase-locked loop (PLL) system, which uses rotor voltages and currents in the proposed method, and is independent of machine parameters, according to the authors. In [7], the operation of the four MRAS-based observers, which are designed for use in DFIGs, are evaluated. These four observers differ in terms of state variables. Since both rotor- and stator-measured parameters can be used in the input vector of the observers, both rotor and stator flux estimation can be used as state variable, based on input variables. In [8], another MRAS observer is presented for DFIMs. Its main property is direct estimation of torque and rotor flux components. Additionally, sensitivity analysis and stability of the suggested method are presented in [8]. The presented algorithm in [9] is relatively simple, and it is not necessary to flux calculations. Its main advantage is reducing the undesired effects of integrators. In [10], another MRAS is proven for DFIM, where a constant gain is considered in the adjustable model of the MRAS to solve the drift problems of the integrators. In [11], an adaptive observer for sensorless control of DFIG is designed that extends the basic Luenberger algorithm for use in DFIG. The proposed MRAS observer of [12] is based on neural networks. In the MRAS observer, introduced in [13], a new adaptation mechanism is applied based on machine reactive power. In [14], a reduced-order adaptive observer is presented for stator flux and speed estimation. In [15], a conventional Kalman filter structure that also uses rotor side measurements is changed to be applied in the sensorless control of DFIM. A straightforward algorithm, without need to flux calculations and integrators, is presented in [16] for rotor position estimation. Speed estimation from slip is presented in [17], which is a developed form of a basic method applied in the sensorless control of DFIG. In [18], a new reduced-order adaptive observer, based on fundamental Luenberger observer, is designed for DFIG and utilizes different state variables. In [19], MRAS control strategy is used to calculate the rotor position and speed, where the air-gap electromotive force (EMF) is taken as the working variable.

According to widely reported works in the literature, observers have proved to be a more acceptable operation, especially with the state variables that use rotor-side measurements in their calculations. This paper presents a new speed estimation algorithm that is based on reduced-order observers and uses rotor-side measurements for the calculation of state variables. The stability of the proposed method is proven with extensive formulation in the design procedure. Both classic and fuzzy PI blocks are considered to be used in the observer structure. Rotor currents and stator fluxes are considered as state variables of the proposed method, and error of the stator flux estimation is used for observer correction and stability analysis. Although the suggested algorithm has weak dependency on the machine parameters, a parameter correction method is presented for machine parameters that may have more influence on the observer operation. Compared to similar works, the introduced combinations are presented for the first time in this paper. The main contributions of the suggested method are as follows. Firstly, the proposed algorithm is reduced-order, which means that it can be implemented simply. Secondly, the adaptation mechanism contains no integrator and derivate operator; therefore, its implementation is relatively simple with fast dynamics. Thirdly, gain matrix calculation and stability analysis are considered on the basis of pole-zero placement, which is a classic control method. Finally, the suggested method for parameter estimation is straightforward.

This paper is organized as follows. In Section 2, a dynamic model of DFIG is presented. The proposed observer structure is described in Section 3. Section 4 presents the proposed parameter estimation algorithm. The simulation and practical results are presented in Sections 5 and 6, respectively, and concluding remarks are given in Section 7.

2. Dynamic modelling of DFIG

A dynamic model of DFIG in dq-axes reference frame is presented in the synchronous reference frame. The voltage equations of a DFIG in an arbitrary reference frame are expressed as follows:

$$\mathbf{V_{sdq}} = R_s \mathbf{i_{sdq}} + \frac{d\psi_{\mathbf{sdq}}}{dt} + j\omega\psi_{\mathbf{sqd}} \tag{1}$$

$$\mathbf{V_{rdq}} = R_r \mathbf{i_{rdq}} + \frac{d\psi_{\mathbf{rdq}}}{dt} + j\left(\omega - \omega_r\right)\psi_{\mathbf{rqd}}, \tag{2}$$

where

$$\psi_{\mathbf{sdq}} = L_s \mathbf{i_{sdq}} + L_m \mathbf{i_{rdq}} \tag{3}$$

$$\psi_{\mathbf{rdq}} = L_r \mathbf{i_{rdq}} + L_m \mathbf{i_{sdq}}, \tag{4}$$

where R_s, R_r, L_s, L_r, and L_m are stator resistance, rotor resistance, stator inductance, rotor inductance, and magnetizing inductance, respectively, and ψ_s, i_r, v_s, and v_r are stator fluxes, rotor currents, stator voltages, and rotor voltages, respectively. Additionally, ω is the arbitrary reference frame speed, which can be considered synchronous speed, and ω_r is the rotor electrical speed. Figure 1 shows the equivalent circuit of a DFIG in the dq frame, described by Eqs. (1)–(4) [20–21]. By substituting Eq. (4) with Eq. (2), and assuming stator fluxes ($\psi_{\mathbf{s}}$) and rotor currents ($\mathbf{i_r}$) as state variables, the basic model of DFIG in state equation form can be rewritten as follows:

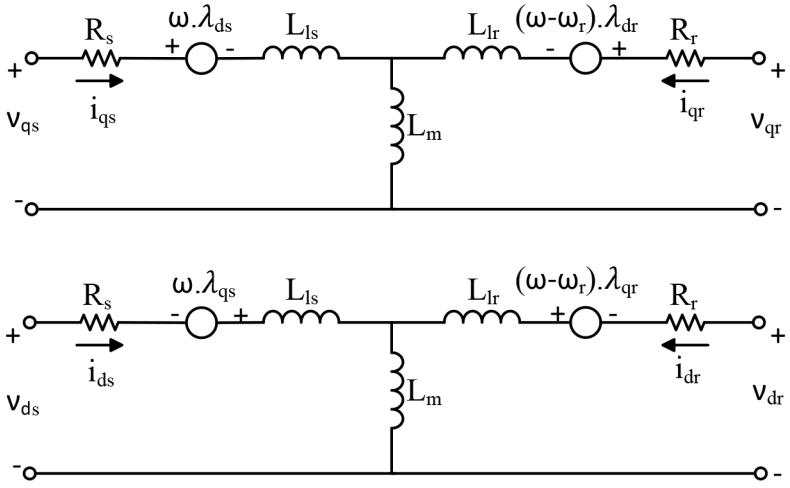

Figure 1. DFIG equivalent circuit in arbitrary reference frame [20,21].

$$\dot{\mathbf{x}} = \mathbf{A}\mathbf{x} + \mathbf{B}\mathbf{u} \tag{5}$$

where

$$\frac{d}{dt}\begin{bmatrix} \psi_s \\ \mathbf{i}_r \end{bmatrix} = \begin{bmatrix} \mathbf{A}_{11} & \mathbf{A}_{12} \\ \mathbf{A}_{21} & \mathbf{A}_{22} \end{bmatrix}\begin{bmatrix} \psi_s \\ \mathbf{i}_r \end{bmatrix} + \begin{bmatrix} \mathbf{B}_{11} & \mathbf{B}_{12} \\ \mathbf{B}_{21} & \mathbf{B}_{22} \end{bmatrix}\begin{bmatrix} \nu_s \\ \nu_r \end{bmatrix}, \tag{6}$$

$$\begin{cases} \mathbf{A}_{11} = -a_5\mathbf{I} + \mathbf{J}\omega_s & \mathbf{A}_{12} = a_6\mathbf{I} \\ \mathbf{A}_{21} = a_1\mathbf{I} + \mathbf{J}a_2\omega_r & \mathbf{A}_{22} = -a_3\mathbf{I} - \mathbf{J}\omega_{sl} \end{cases} \tag{7}$$

$$\begin{cases} \mathbf{B}_{11} = \mathbf{I} & \mathbf{B}_{12} = \mathbf{O} \\ \mathbf{B}_{21} = -a_2\mathbf{I} & \mathbf{B}_{22} = a_4\mathbf{I} \end{cases} \tag{8}$$

and

$$\sigma = 1 - \frac{L_m^2}{L_r L_s} \tag{9}$$

$$a_1 = \frac{L_m}{\tau_s \sigma L_s L_r} \tag{10}$$

$$a_2 = \frac{1-\sigma}{L_m \sigma} \tag{11}$$

$$a_3 = \left(\frac{1-\sigma}{\sigma\tau_s} + \frac{1}{\sigma\tau_r}\right) \tag{12}$$

$$a_4 = \frac{1}{\sigma L_r} \tag{13}$$

$$a_5 = \frac{1}{\tau_s} \tag{14}$$

$$a_6 = \frac{L_m}{\tau_s} \tag{15}$$

where $\mathbf{A}$ is state matrix, $\mathbf{B}$ is input matrix, $I = diag(1,1)$ is a unit matrix, and $\mathbf{O}$ is a zero matrix from second order. Furthermore,

$$\mathbf{i}_r = \begin{bmatrix} i_{dr} & i_{qr} \end{bmatrix}^T \tag{16}$$

$$\psi_s = \begin{bmatrix} \psi_{ds} & \psi_{qs} \end{bmatrix}^T \tag{17}$$

$$\mathbf{u} = \begin{bmatrix} \nu_s & \nu_r \end{bmatrix}^{\mathbf{T}} \tag{18}$$

$$\nu_s = \begin{bmatrix} \nu_{ds} & \nu_{qs} \end{bmatrix}^T \tag{19}$$

$$\nu_r = \begin{bmatrix} \nu_{dr} & \nu_{qr} \end{bmatrix}^T \tag{20}$$

Furthermore, the electrical torque equation of DFIG is as presented below:

$$T_{em} = \frac{3}{2} P \frac{L_m}{L_s} Im\left\{\psi_s i_r^*\right\}, \tag{21}$$

where P is the pole pairs of the machine.

3. Description of the proposed observer structure

This section describes an adaptive observer, based on a real-time estimation of the stator flux. Rotor speed can be estimated by using an adaptation mechanism. In the suggested observer, real-time measurements of the DFIG voltages and currents are needed. Stator flux and rotor current vectors are selected as state variables in the structure of the proposed observer. The error between the estimated and calculated values of the stator flux is applied to correct the DFIG model according to the reference model. For this purpose, the error value is multiplied in a gain matrix, $\boldsymbol{L}$, and then the resulting signal is used as nonlinear feedback to correct the observer state matrix.

3.1. Main structure

Based on the DFIG model, explained in Section 2, and considering error correction term, the suggested reduced-order observer is given by

$$\dot{\hat{\mathbf{x}}} = \hat{\mathbf{A}}\hat{\mathbf{x}} + \mathbf{B}\mathbf{u} - \mathbf{L}(\psi_{\mathbf{s}} - \hat{\psi}_{\mathbf{s}}) \tag{22}$$

$$\frac{d}{dt}\hat{\psi}_s = \mathbf{A}_{11}\hat{\psi}_s + \mathbf{A}_{12}\mathbf{i}_r + \mathbf{B}_{11}\nu_s - \mathbf{L}\left(\psi_{\mathbf{s}} - \hat{\psi}_{\mathbf{s}}\right) \tag{23}$$

The sign $\wedge$ denotes the estimated parameters. In Eqs. (22) and (23), $L = \begin{bmatrix} L_{11} & L_{12} \\ L_{21} & L_{22} \end{bmatrix}$ is the gain matrix of the observer. The gain matrix design, which will be explained in the next section, must warrant the observer stability.

Since the direct measurement of stator flux $\psi_{\mathbf{s}}$ needs special sensors placed in the machine windings, the real value of $\psi_{\mathbf{s}}$ is calculated as follows:

$$\psi_{\mathbf{s}} = L_s\mathbf{i}_s + L_m\mathbf{i}_r e^{-j\theta_{sl}} \tag{24}$$

In Eq. (24), real-time measurements of stator and rotor currents are needed. Furthermore, the rotor current must be transformed to the stator reference frame. Therefore, slip angle $\theta_{sl} = \theta_s - \theta_r$ is needed, where $\theta_s = \int \omega_s dt$ and $\theta_r = \int \omega_r dt$. In sensorless vector-controlled systems, estimated values can be used where $\hat{\theta}_r = \int \hat{\omega}_r dt$. Using Eqs. (23) and (24), a reduced-order observer can be designed, and its general block diagram is illustrated in Figure 2.

3.2. Design of gain matrix

The stability of the observer must be ensured by proper design of its gain matrix. Stability conditions can be proven according to the error dynamics. By subtracting Eq. (23) from Eq. (6), the error dynamics can be obtained as follows:

$$\begin{aligned} \tfrac{d}{dt}\left(\psi_s - \hat{\psi}_s\right) &= \mathbf{A}_{11}\psi_s + \mathbf{A}_{12}\mathbf{i}_r + \mathbf{B}_{11}\nu_s - \mathbf{A}_{11}\hat{\psi}_s - \mathbf{A}_{12}\mathbf{i}_r - \mathbf{B}_{11}\nu_s + \mathbf{L}\left(\psi_s - \hat{\psi}_s\right) \\ &= \mathbf{A}_{11}\left(\psi_s - \hat{\psi}_s\right) + \mathbf{L}\left(\psi_s - \hat{\psi}_s\right) = (\mathbf{A}_{11} + \mathbf{L})\left(\psi_s - \hat{\psi}_s\right) \end{aligned} \tag{25}$$

Therefore,

$$\dot{\mathbf{e}} = (\mathbf{A}_{11} + \mathbf{L})\,\mathbf{e}, \tag{26}$$

where $\mathbf{e} = \left(\psi_s - \hat{\psi}_s\right)$ is the established error between stator flux-calculated and estimated values.

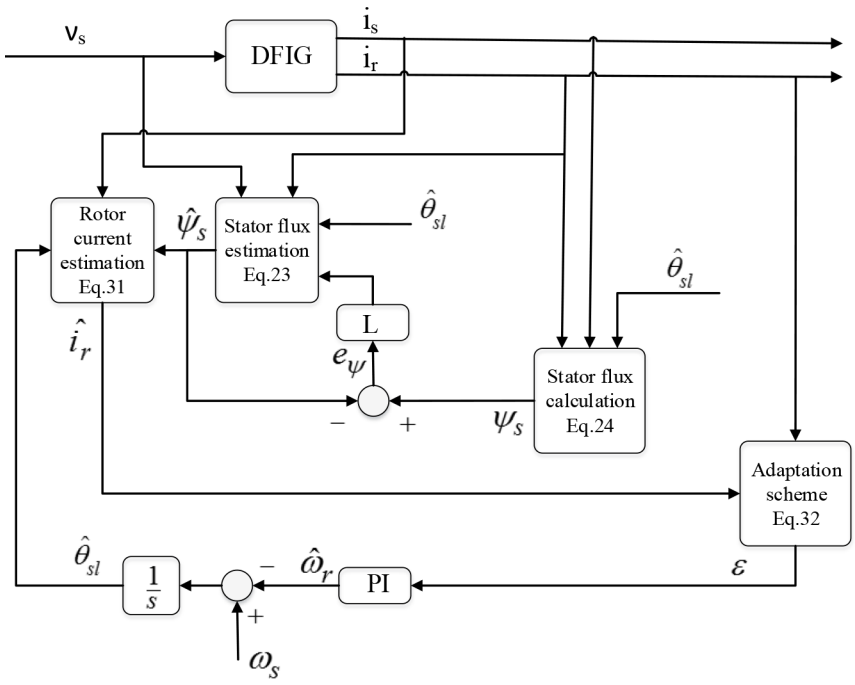

Figure 2. Proposed reduced-order adaptive speed observer.

In order to achieve stable operation for the suggested observer, the dynamics of the estimation error must be asymptotically stable. Therefore, gain matrix $\boldsymbol{L}$ must be selected in a procedure in which $(A_{11}+L)$ is a Hurwitz matrix. In other words, real parts of $(A_{11}+L)$ eigenvalues must be negative. $(A_{11}+L)$ is assumed to be a diagonal matrix, as follows:

$$\mathbf{A}_{11}+\mathbf{L}=\begin{bmatrix}\beta_d & 0\\ 0 & \beta_q\end{bmatrix}, \tag{27}$$

where $\beta_d<0$ and $\beta_q<0$ are the desired eigenvalues. Therefore,

$$\mathbf{L}=\begin{bmatrix}\beta_d & 0\\ 0 & \beta_q\end{bmatrix}-\begin{bmatrix}-a_5 & -\omega_s\\ \omega_s & -a_5\end{bmatrix} \tag{28}$$

After simplification, we have

$$\begin{bmatrix}L_{11} & L_{12}\\ L_{21} & L_{22}\end{bmatrix}=\begin{bmatrix}\beta_d+a_5 & \omega_s\\ -\omega_s & \beta_q+a_5\end{bmatrix} \tag{29}$$

By selecting correction gain as (29), $e=0$ is an asymptotically stable equilibrium point. Convergence speed is determined by β_q and β_d amounts; β_q and β_d must be selected as big enough.

3.3. Adaptation mechanism

Rotor current real and estimated values are used in the adaptation mechanism of the proposed observer. Rotor current can be obtained by rewriting Eq. (24) as follows:

$$\mathbf{i}_r=e^{j\theta_{sl}}\frac{(\psi_s-L_s\mathbf{i}_s)}{L_m} \tag{30}$$

Now, by applying stator flux from Eq. (23) instead of $\psi_{\mathbf{s}}$, the estimated value of the rotor current in the rotor reference frame can be obtained as follows:

$$\hat{\mathbf{i}}_r = e^{j\hat{\theta}_{sl}} \frac{\left(\hat{\psi}_s - L_s \mathbf{i}_s\right)}{L_m}, \tag{31}$$

where $\hat{\theta}_{sl} = \theta_s - \hat{\theta}_r$.

As mentioned previously, by comparing rotor-current estimated and measured values and calculating the angular difference between them, rotor speed and position can be estimated. However, the angular difference varies in a wide range $(-\pi, \pi)$; therefore, its determination is difficult [11]. Cross product between estimated and measured vectors of rotor current is a solution to determining the considered angular difference. Therefore,

$$\begin{aligned} \varepsilon &= \hat{i}_{dr} i_{qr} - i_{dr} \hat{i}_{qr} \\ \varepsilon &= \hat{\mathbf{i}} \times \mathbf{i} \end{aligned}, \tag{32}$$

where $\left(\hat{i}_{dr}, \hat{i}_{qr}, i_{dr}, i_{qr}\right)$ are the rotor current's measured and estimated values in the rotor reference frame. The resulting error is passed through a PI block to estimate rotor speed.

$$\hat{\omega}_r = K_{P\omega}\varepsilon + K_{I\omega} \int \varepsilon dt \tag{33}$$

Integration of the estimated speed leads to an estimation from rotor position, as follows:

$$\hat{\theta}_r = \int \hat{\omega}_r dt \tag{34}$$

3.4. Fuzzy proportional integrator

The applied PI in Eq. (29) can be replaced by a fuzzy-based PI. Fuzzy controller is an input/output static nonlinear mapping. Therefore, a PI control action can be formulated as follows [22]:

$$K_1.E + K_2.dE = dU, \tag{35}$$

where K_1 and K_2 are nonlinear coefficients, E is the error signal, and U is the control signal. By integration of Eq. (35), we have

$$U = K_1. \int Edt + K_2.E, \tag{36}$$

which is a fuzzy PI control with nonlinear coefficients. A fuzzy PI controller is depicted in Figure 3. A sample of fuzzy sets can be defined as follows:

Z = zero, PB = positive big, NB = negative big, PS = positive small, NS = negative small, PVS = positive very small, PM = positive medium, NM = negative medium, NVS = negative very small.

Therefore, the suggested rule matrix is considered as in Table 1. Finally, the explained fuzzy PI can be applied instead of the conventional PI of Figure 2.

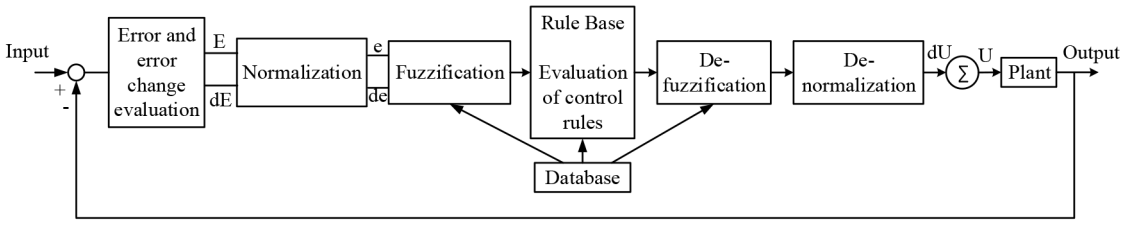

Figure 3. Fuzzy PI model [22].

Table 1. Sample rule matrix.

And		e (p.u.)							
		NB	NM	NS	Z	PS	PM	PB	
de (p.u.)	NB	*NVB*	*NVB*	*NVB*	*NB*	*NM*	*NS*	*Z*	***du (p.u.)***
	NM	*NVB*	*NVB*	*NB*	*NM*	*NS*	*Z*	*PS*	
	NS	*NVB*	*NB*	*NM*	*NS*	*Z*	*PS*	*PM*	
	Z	*NB*	*NM*	*NS*	*Z*	*PS*	*PM*	*PB*	
	PS	*NM*	*NS*	*Z*	*PS*	*PM*	*PB*	*PVB*	
	PM	*NS*	*Z*	*PS*	*PM*	*PB*	*PVB*	*PVB*	
	PB	*Z*	*PS*	*PM*	*PB*	*PVB*	*PVB*	*PVB*	
		du (p.u.)							

4. Parameter estimation for proposed observer

It is well known that machine parameters vary due to temperature rises and magnetic saturation [23]. Any variation in machine parameters, such as inductances, may disturb the speed estimation of the observer. Accurate estimation needs perfect data from machine parameters. Since the proposed reduced-order observer is on the basis of stator flux, parameter mismatch effects on the estimated speed must be considered. Therefore, this section describes a straightforward parameter correction method. The main property of the suggested method is its simplicity.

Stator, rotor, and magnetic inductances (L_s, L_r, L_m) are effective parameters in the stator flux and rotor current estimation. The introduced method for parameter estimation is based on the equations of stator and rotor fluxes. We have

$$\lambda_r = L_r i_r + L_m i_s \tag{37a}$$

$$\lambda_s = L_s i_s + L_m i_r \tag{37b}$$

On the other hand, it is assumed that stator, rotor, and magnetic inductances change at the same rate [24]. Therefore,

$$\frac{\hat{L}_s}{L_s} = \frac{\hat{L}_r}{L_r} = \frac{\hat{L}_m}{L_m} = \Gamma, \tag{38}$$

where L_s, L_r, and L_m are nominal values of stator, rotor, and magnetic inductances, and $\left(\hat{L}_s, \hat{L}_r, \hat{L}_m\right)$ are their estimated values, respectively. Extracting rotor current, $\mathbf{i_r}$, from Eq. (37a) and replacing it with Eq. (37b) leads to

$$\lambda_s - \frac{L_m}{L_r}\lambda_r = L_s \sigma i_s \tag{39}$$

From Eqs. (38) and (39), we have

$$\Gamma = \frac{\lambda_s - (L_m/L_r)\,\lambda_r}{\sigma L_s i_s} \tag{40}$$

It should be noted that $\lambda_{\mathbf{s}}$ and $\lambda_{\mathbf{r}}$ are estimated values and $\mathbf{i_s}$ is measured using current sensors. Additionally,

$$\hat{\lambda}_r = \left(a_2\lambda_s + \hat{i}_r\right)\Big/ a_4 \tag{41}$$

Figure 4 depicts the proposed parameter estimation method.

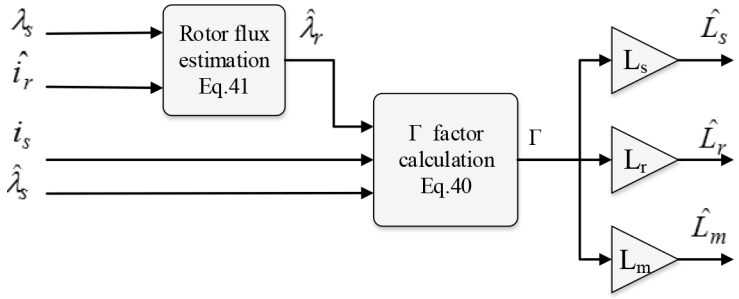

Figure 4. Proposed straightforward parameter correction algorithm.

5. Simulation results

Speed tracking of the proposed method is confirmed by the simulation results, which are presented in this section. A 1.5-MW DFIG is simulated using MATLAB/Simulink and its parameters are presented in Table 2. Figure 5 shows the speed-tracking capability of the proposed adaptive observer, where wind speed ranges from 9 to 15 m/s. Active and reactive powers of DFIG are depicted in the same figure. Active power ranges from 0.92 (for wind speed of 15 m/s) to 0.78 p.u. (for a wind speed of 9 m/s). Reactive power is set to be zero by the controller, which, after some oscillations in the beginning, settles on zero. This proves the effective operation of the controller. Furthermore, as can be seen, speed estimation error varies around zero with an amplitude of less than 0.1. Rotor current estimation quality is shown in Figure 6. As can be seen, the produced error of the suggested method is less than 0.05 p.u.; therefore, speed tracking is acceptable.

Table 2. Parameters of the simulated DFIG.

Nominal power	1.5 MW
Nominal voltage	575 V
Frequency	50 Hz
R_s	0.023 p.u.
L_{is}	0.18 p.u.
R_r	0.016 p.u.
L_{ir}	0.16 p.u.
L_m	2.9 p.u.
Pairs of poles	1
Moment of inertia	0.685 kg.m^2

Speed tracking with the suggested fuzzy PI is illustrated in Figure 7. Compared to Figure 5, the established estimation error with the fuzzy PI is more than the error of the conventional PI. Although it complicates the controller, to reduce the error it is required to use many more rules than the current state.

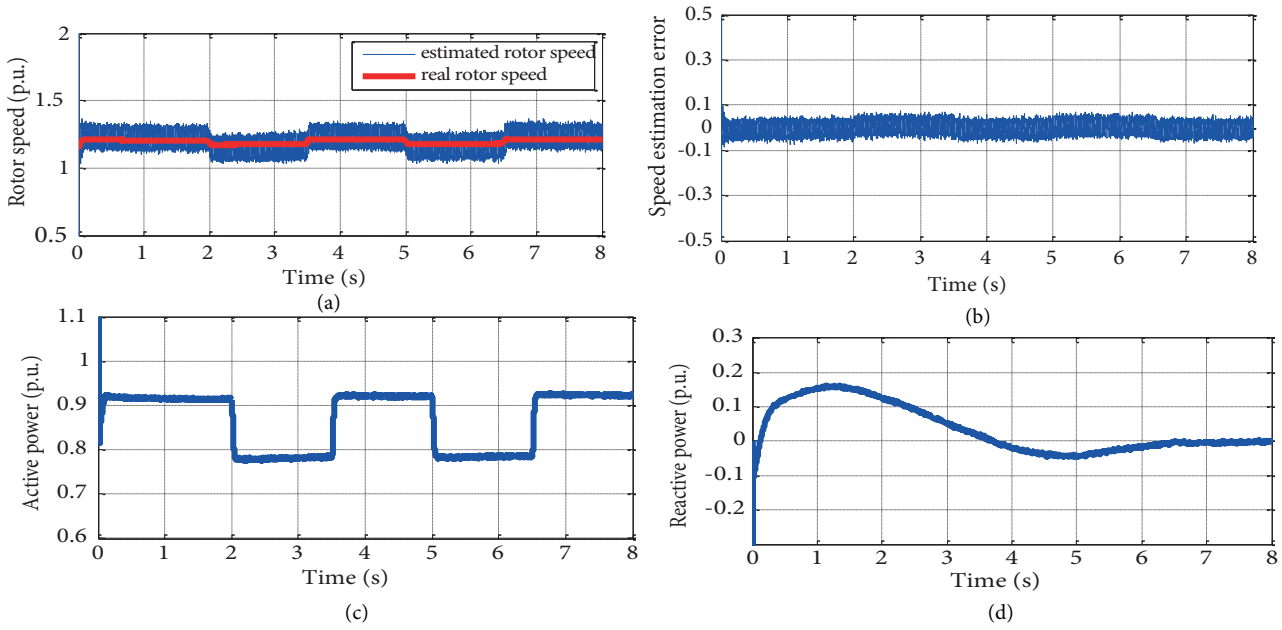

Figure 5. Speed tracking capability of proposed observer. a) Real and estimated speed, b) estimation error, c) active power variations, d) reactive power variations.

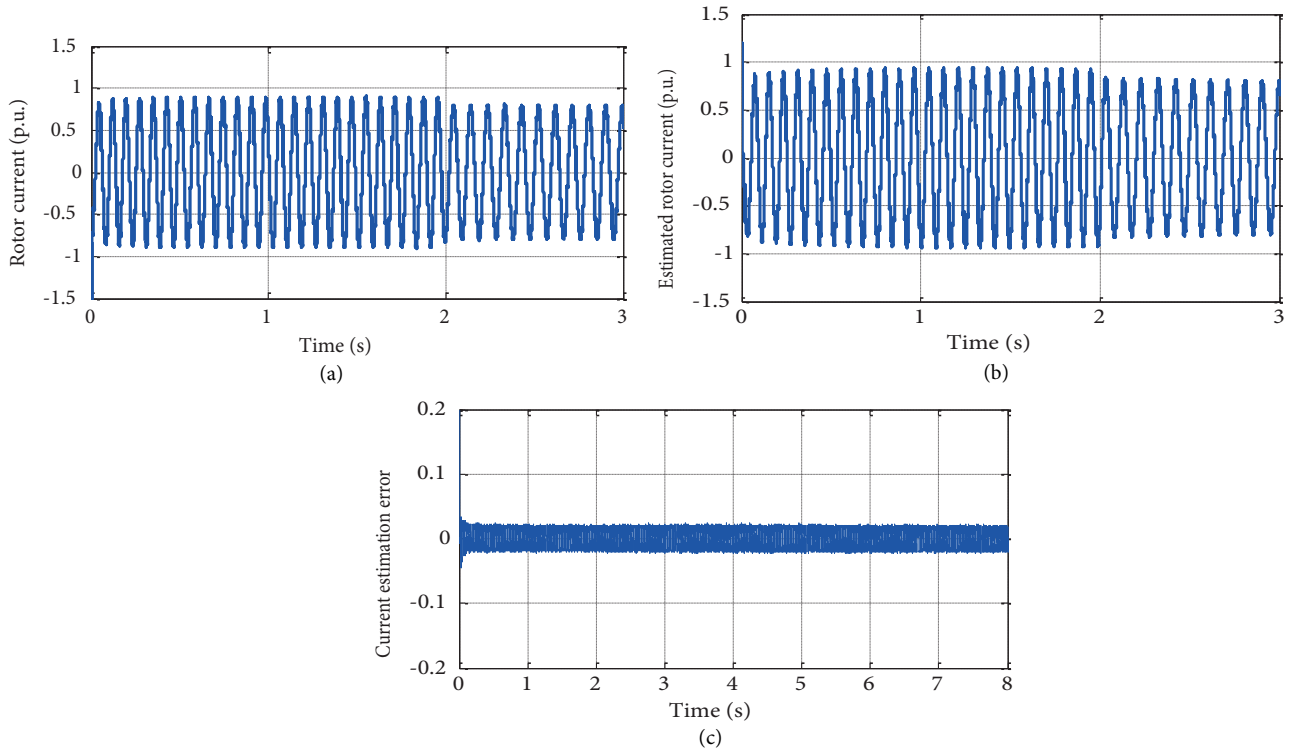

Figure 6. a) Measured rotor current, b) estimated rotor current, c) estimation error.

Speed observer operation is also verified when voltage sag occurs. In the considered voltage sag, illustrated in Figure 8, voltage amplitude decreases from 1 to 0.9 p.u. for about 0.4 s. This can be seen despite the estimated speed oscillation in the voltage variations, but it tracks the real speed with acceptable estimation error.

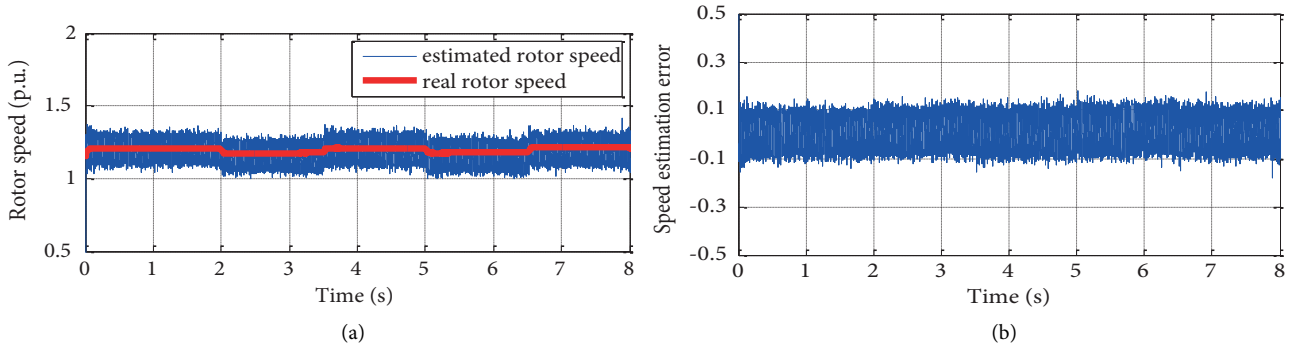

Figure 7. Speed tracking capability of proposed observer with fuzzy PI: a) real and estimated speed, b) estimation error.

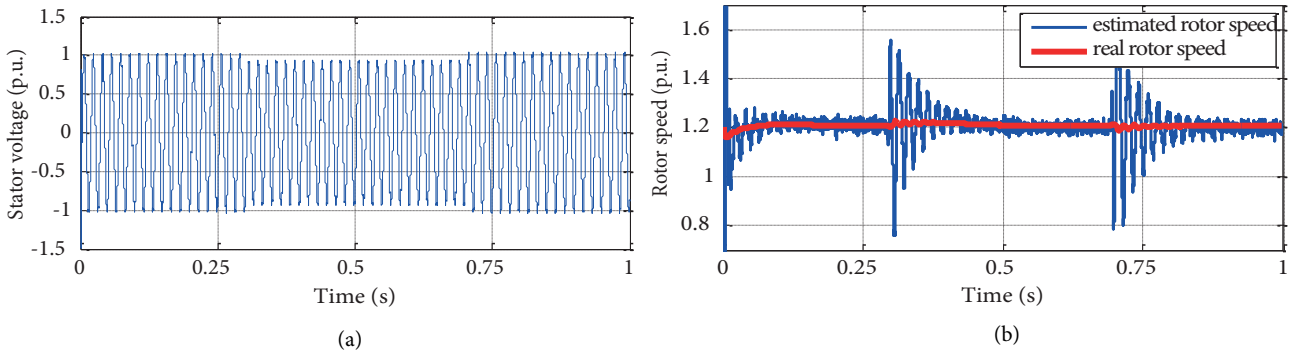

Figure 8. Observer operation in the voltage sag condition: a) DFIG terminal voltage variations, b) real and estimated speed.

Speed tracking is also examined in a subsynchronous speed area. In Figure 9, wind speed changes from 15 m/s to 6 m/s. Although the estimation error is increased in the subsynchronous operation of the DFIG, it can be proved that the estimated speed can track the real speed.

Parameter correction for the suggested observer is also simulated in this section. Figure 10 shows parameter estimation for mutual, stator, and rotor inductances, where parameter estimation error for each of the considered parameters is acceptable.

6. Practical results

Some dynamic behaviors of the suggested method are proven using a laboratory setup consisting of (1) a DC motor that plays the role of a wind turbine; (2) a wound rotor induction machine (WRIM); (3) a 16-bit dspIC30F4011 digital controller and firing units for switching of the IGBTs [25]; and (4) PCI-1716 and PCLD-8710 I/O boards for real-time evaluation of the suggested algorithm. The DFIG parameters are presented in Table 3 and Figure 11 shows the general block diagram of the experimental setup. The firing units contain an isolated power supply and a control circuit based on HCPL316j IC for each IGBT. Therefore, each firing unit consists of 12 isolated power supplies and 12 control circuits. Programming language for the digital controller is C. The controller generates firing signals for the related units, and the aim of controlling the rotor-side converter is to control machine speed and limit harmonic content of rotor currents. On the other hand, the aim of controlling the grid-side converter is to fix DC-link voltage and control active and reactive powers. Some required measurements from machine and converters terminals are loaded to a computer via the above-

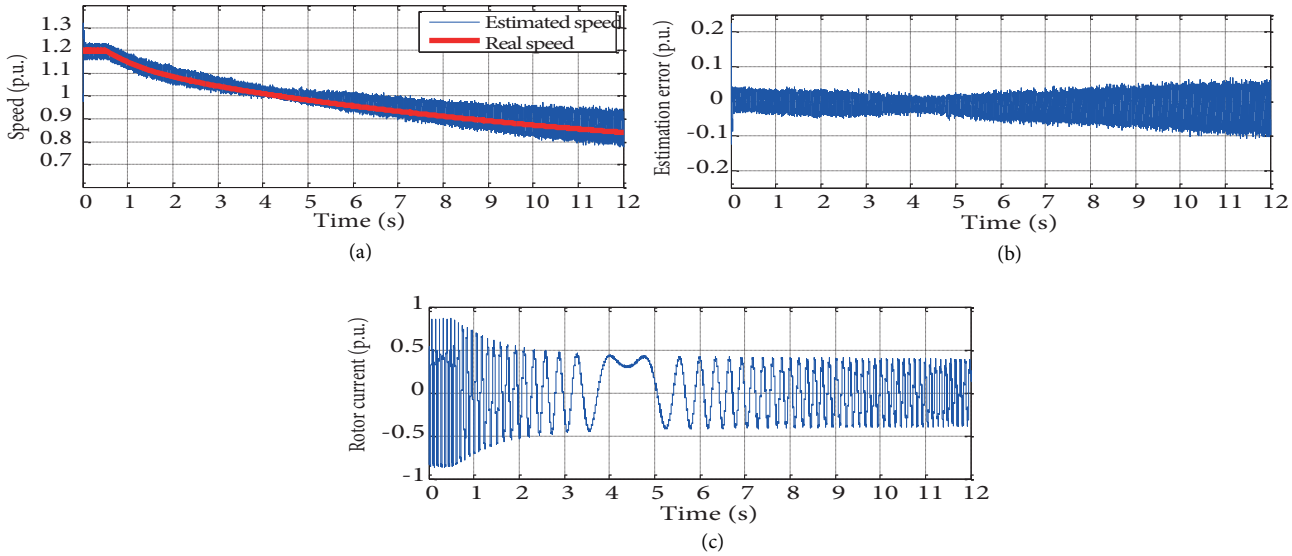

Figure 9. Observer operation in the sub-synchronous operation area: a) real and estimated speed, b) estimation error, c) rotor current variations in Phase A.

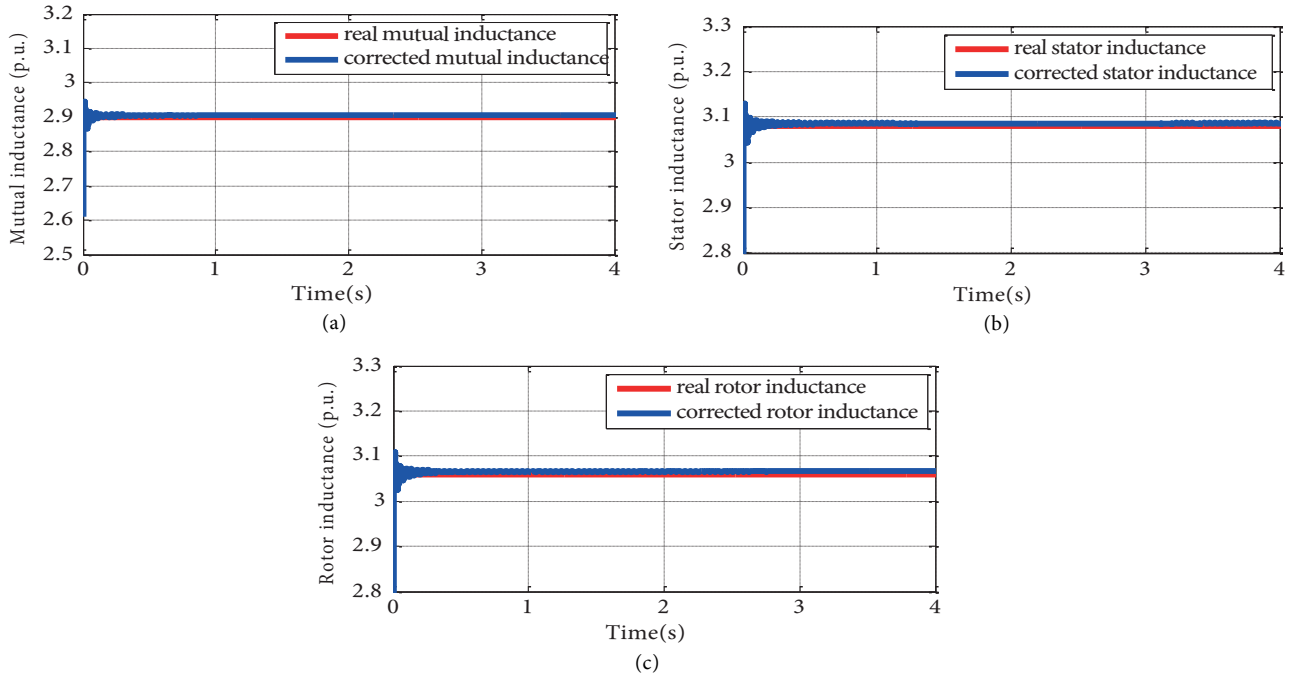

Figure 10. Estimation of DFIG parameters: a) mutual inductance, b) stator inductance, c) rotor inductance.

mentioned I/O boards, which are used for real-time evaluation of the proposed estimation algorithms. Machine control and generation of firing signals is implemented by the digital controller [26].

Steady state operation of the DFIG is illustrated in Figure 12, where speed is fixed at 3500 rpm. Nominal speed of the machine is 3000 rpm, and machine speed is increased using a DC machine. Therefore, the IM is in generator mode. The rotor current of the IM is depicted in the same figure. It shows the controller performance in successful control of the machine speed and rotor currents. Speed tracking of the observer is depicted in

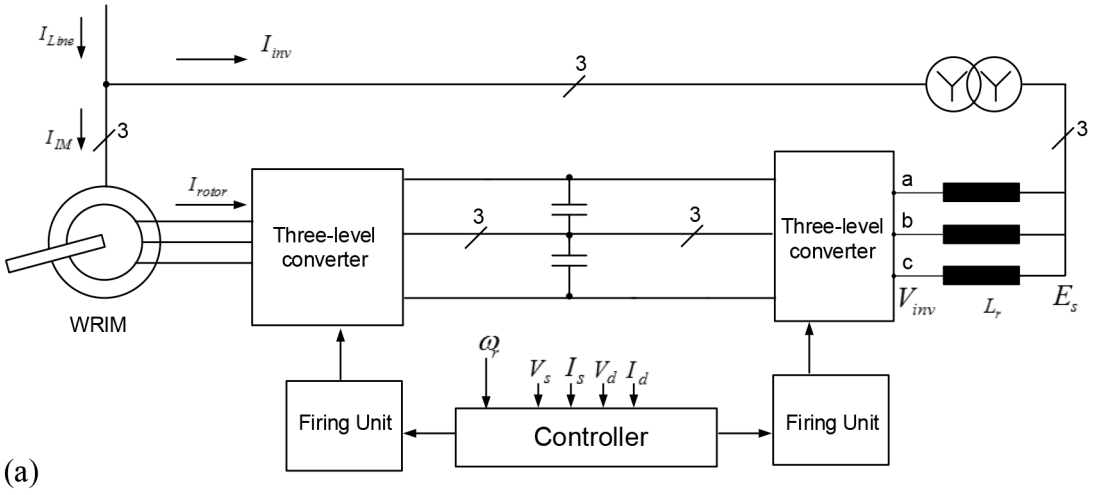

(a)

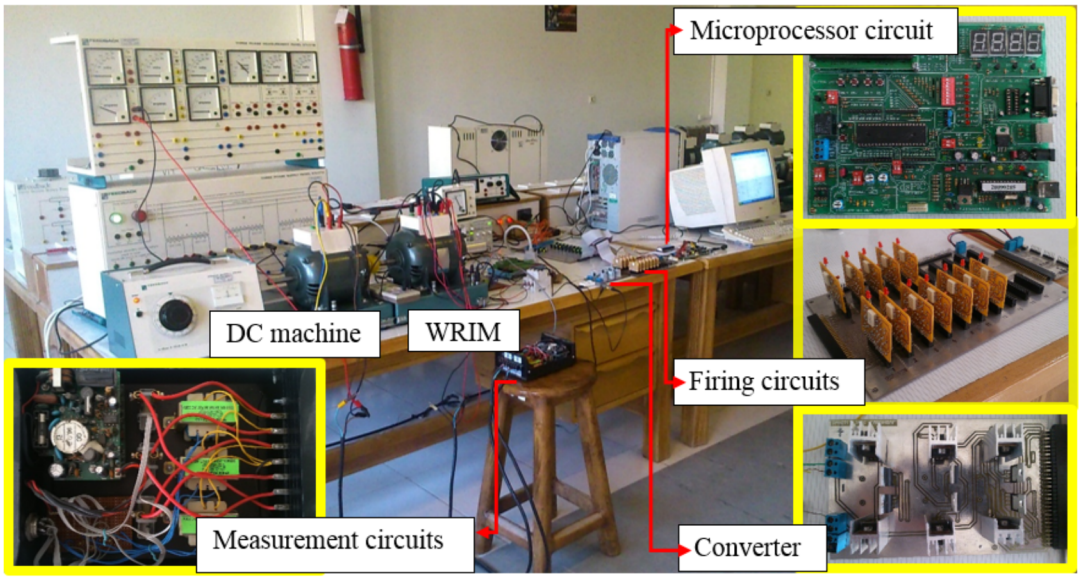

(b)

Figure 11. Laboratory setup: a) general block diagram, b) constructed circuits.

Table 3. Parameters of the DFIG, used for practical results.

Nominal power	0.25 kW
Nominal voltage	120 V
Frequency	50 Hz
R_s	1.7 Ω
L_{is}	0.012 H
R_r	1.6 Ω
L_{ir}	0.012 H
L_m	0.379 H
Pairs of poles	1
Moment of inertia	0.03 kg.m^2

Figure 13, where speed changes from 3000 to 3500 rpm. Moreover, the real-time speed tracking capability of the observer under practical conditions is acceptable with proper ripple and dynamic.

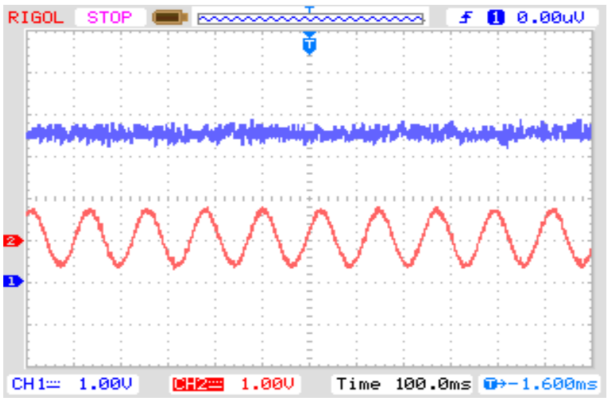

Figure 12. Steady state operation of the DFIG (upper: speed, and lower: rotor current) (CH1: 1000 rpm/div. CH2: 1 A/div.).

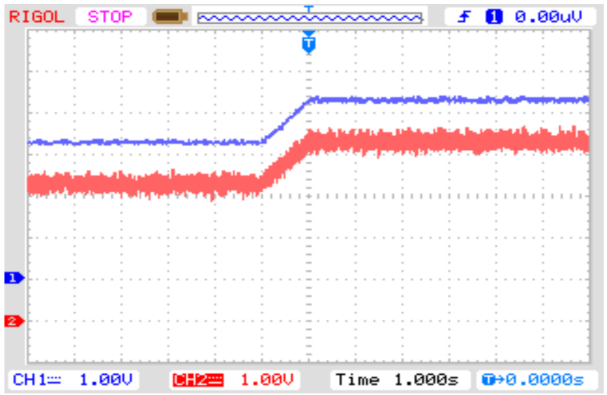

Figure 13. Speed tracking capability of the proposed observer under practical conditions (upper: real speed, and lower: estimated speed) (CH1 and CH2: 1000 rpm/div.).

7. Conclusion

This paper introduced and analyzed a novel adaptive observer, which is based on the concepts of the Luenberger algorithm. In the suggested observer, rotor current and stator flux were selected as state variables of the DFIG model. Stator flux error was used to correct the estimation equation of the observer, and rotor current was used to extract the adaptation mechanism of the proposed observer. Moreover, the gain matrix of the suggested observer was designed for obtaining stable operation, where a complete analysis of error dynamics was presented. The main specification of the proposed observer is its high-quality speed tracking with fast dynamic, and, under several conditions such as fast variations of the wind speed, its subsynchronous operation area and transient fault conditions, i.e. voltage sag. Furthermore, an analytical method was verified for parameter correction of the suggested observer. Simulation results were obtained to prove the proposed observer speed tracking capability and parameter correction quality. Finally, some dynamic behaviors of the observer were examined using a practical setup, which is based on a 16-bit DSPIC architecture.

References

[1] Wang Z, Li G, Sun, Boon TO. Effect of erroneous position measurements in vector-controlled doubly fed induction generator. IEEE T Energy Conver 2010; 25: 59-69.

[2] Zin AAM, Naderipour A, Bin-Habibuddin MH, Guerrero JM. Harmonic currents compensator GCI at the microgrid. Electron Lett 2016; 52: 1714-1715.

[3] Naderipour A, Zin AAM, Bin-Habibuddin MH. Improved power-flow control scheme for a grid-connected microgrid. Electron World 2016; 122: 42-45.

[4] Vas P. Sensorless Vector and Direct Torque Control. Oxford, UK: Oxford University Press, 1998.

[5] Cardenas R, Pena R, Proboste J, Asher G, Clare J. MRAS observer for sensorless control of standalone doubly fed induction generators. IEEE T Energy Conver 2005; 20: 710-718.

[6] Akel F, Ghennam T, Berkouk EM, Laour M. An improved sensorless decoupled power control scheme of grid connected variable speed wind turbine generator. Energ Convers Manage 2014; 78: 584-594.

[7] Cardenas R, Pena R, Clare J, Asher G, Proboste J. MRAS observers for sensorless control of doubly-fed induction generators. IEEE T Power Electr 2008; 23: 1075-1084.

[8] Dezza FC, Foglia G, Iacchetti MF, Perini R. An MRAS observer for sensorless DFIM drives with direct estimation of the torque and flux rotor current components. IEEE T Power Electr 2012; 27: 2576-2584.

[9] Karthikeyan A, Nagamani C, Chaudhury ABR, Ilango GS. Implicit position and speed estimation algorithm without the flux computation for the rotor side control of doubly fed induction motor drive. IET Electr Power App 2012; 6: 243-252.

[10] Iacchetti M, Carmeli MS, Castelli Dezza F, Perini R. A speed sensorless control based on a MRAS applied to a double fed induction machine drive. Electr Eng 2010; 91: 337-345.

[11] Forchetti DG, Garcia GO, Valla MI. Adaptive observer for sensorless control of stand-alone doubly fed induction generator. IEEE T Ind Electron 2009; 56: 4174-4180.

[12] Cortajarena JA, De Marcos J. Neural network model reference adaptive system speed estimation for sensorless control of a doubly fed induction generator. Electr Pow Compo Sys 2013; 41: 1146-1158.

[13] Pattnaik MP, Kastha DK. Adaptive speed observer for a stand-alone doubly fed induction generator feeding nonlinear and unbalanced loads. IEEE T Energy Conver 2012; 27: 1018-1026.

[14] Yongsu H, Sungmin K, Jung-Ik H. Sensorless vector control of doubly fed induction machine using a reduced order observer estimating. In: IEEE 2012 Energy Conversion Congress and Exposition; 15–20 September 2012; Raleigh, NC, USA. New York, NY, USA: IEEE. pp. 2623-2630.

[15] Serhoud H, Benattous D. Sensorless optimal power control of brushless doubly-fed machine in wind power generator based on extended kalman filter. Int J Syst Ass Eng 2013; 4: 57-66.

[16] Karthikeyan A, Nagamani C, Ilango GS. A versatile rotor position computation algorithm for the power control of a grid-connected doubly fed induction generator. IEEE T Energy Conver 2012; 27: 697-706.

[17] Marques GD, Sousa DM. Sensorless direct slip position estimator of a DFIM based on the air gap pq vector-sensitivity study. IEEE T Ind Electron 2013; 60: 2442-2450.

[18] Sheng Y, Ajjarapu V. A speed-adaptive reduced-order observer for sensorless vector control of doubly fed induction generator-based variable-speed wind turbines. IEEE T Energy Conver 2010; 25: 891-900.

[19] Gayen PK, Chatterjee D, Goswami SK. Stator side active and reactive power control with improved rotor position and speed estimator of a grid connected DFIG (doubly-fed induction generator). Energy 2015; 89: 461-472.

[20] Abad G, López J, Rodríguez M, Marroyo L, Iwanski G. Doubly Fed Induction Machine: Modeling and Control for Wind Energy Generation Applications. Hoboken, NJ, USA: Wiley-IEEE Press, 2011.

[21] Martinez MI, Tapia G, Susperregui A, Camblong H. Sliding-mode control for DFIG rotor-and grid-side converters under unbalanced and harmonically distorted grid voltage. IEEE T Energy Conver 2012; 27: 328-339.

[22] Bimal KB. Modern Power Electronics and AC Drives. Upper Saddle River, NJ, USA: Prentice Hall, 2002.

[23] Carmeli MS, Castelli-Dezza F, Iacchetti M, Perini R. Effects of mismatched parameters in MRAS sensorless doubly fed induction machine drives. IEEE T Power Electr 2010; 25: 2842-2851.

[24] Djoudi A, Chekireb H, Bacha S. On-line identification of DFIG parameters with rotor current reconstitution. In: IEEE 2014 International Conference on Ecological Vehicles and Renewable Energies; 25–27 March 2014; Monte Carlo, Monaco. New York, NY, USA: IEEE. pp. 1-6.

[25] Mokhberdoran A, Ajami A. Symmetric and asymmetric design and implementation of new cascaded multilevel inverter topology. IEEE T Power Electr 2014; 29: 6712-6724.

[26] Ajabi-Farshbaf R, Azizian MR, Shazdeh S, Mokhberdoran A. Modelling of a new configuration for DFIGs using T-type converters and a predictive control strategy in wind energy conversion systems. IJRER 2016; 6: 975-986.